Low-Cost Non-Uniform Metallic Lattice for Rectifying Aperture Near-Field of Electromagnetic Bandgap Resonator Antennas

Ali Lalbakhsh, *Member, IEEE*, Muhammad U. Afzal, *Member, IEEE*, Karu P. Esselle, *Fellow, IEEE* and Stephanie L. Smith *Member, IEEE*

***Abstract*—This paper addresses a critical issue, which has been overlooked, in relation to the design of Phase Correcting Structures (PCSs) for Electromagnetic Bandgap (EBG) Resonator Antennas (ERAs). All previously proposed PCSs for ERAs are made either using several expensive Radio Frequency (RF) dielectric laminates, or thick and heavy dielectric materials, contributing to very high fabrication cost, posing an industrial impediment to the application of ERAs. This paper presents a new industrial-friendly generation of PCS, in which dielectrics, known as the main cause of high manufacturing cost, are removed from the PCS configuration, introducing an All-Metallic PCS (AMPCS). Unlike existing PCSs, a hybrid topology of fully-metallic spatial phase shifters are developed for the AMPCS, resulting in an extremely lower prototyping cost as that of other state-of-the-art substrate-based PCSs. The APMCS was fabricated using laser technology and tested with an ERA to verify its predicted performance. Results show that the phase uniformity of the ERA aperture has been remarkably improved, resulting in 8.4 dB improvement in the peak gain of the antenna and improved sidelobe levels (SLLs). The antenna system including APMCS has a peak gain of 19.42 dB with a 1-dB gain bandwidth of around 6%.**

***Index Terms*—All-metal manufacturing, Electromagnetic Band Gap (EBG) Resonator Antenna, electromagnetic near-field distribution, Fabry-Perot resonator antenna, frequency selective surfaces, high gain, laser cutting prototyping, metasurface, phase correction, Phase Correcting Surface (PCS), Resonant Cavity Antenna (RCA).**

I. Introduction

In modern communication systems, directive antennas play an essential role in various applications such as satellite reception, point to point microwave links and back-haul networks. Reflector antennas are perhaps considered as one of the most conventional directive antennas with stable radiation patterns [1]; however their parabolic shapes along with their large sizes become problematic in some applications, such as communication on-the-move. Another category of the narrow-beam antennas are array antennas which occupy considerably less space; however a complex feed network is required which potentially increases the loss throughout the antenna system, and the fabrication cost. The third category of the directive antennas are cavity-based antennas, such as electromagnetic bandgap (EBG) Resonators Antennas (ERAs) also known as resonant cavity antennas and Febry-Perot resonator antennas which have the advantage of a single feed and a planar structure [2]–[8]. Despite the mentioned desired ERAs' characteristics, the near-field phase defect of this class of antenna was revealed in 2015 [9] and since then, several solutions have been proposed to tackle this deficiency in the hope of making ERAs a practical solution, when volumetric features along with electromagnetic characteristics are critical [9]–[20]. It is important to re-iterate that the lens theory cannot be applied on ERAs or any similar antennas to estimate their phase errors, as neither of the two essential conditions of single point source and reflection-free medium is satisfied in relation to ERAs, as explicitly discussed in [9], [10]. As a result, the first generation of Phase Correcting Structure (PCS) for ERAs was proposed and tested successfully, suggesting significant improvement in the near-field phase uniformity, leading to highly directive radiation patterns with stable side lobe levels [9]. This very first class of PCS is composed of several dielectric heights to effectively manipulate the local aperture-phase values for phase-error minimization at the operating frequency [9]–[11]. However, the non-planar configuration, very high fabrication cost, as well as undesirably heavy weight of such PCSs were a serious impediment to fully introduce the modified ERAs as a viable industrially justified solution. To mitigate some of these issues, semi-planar configurations were later on proposed, in which high-profile single-dielectric in the PCS configurations was replaced by composite-based dielectrics, leading to a lighter PCS with a smaller profile at the expense of more complex fabrication process [14].

The second generation of PCS has been recently introduced [12], [13], [15], in which undesirably thick phase-correcting regions, in the first generation, have been replaced by completely planar metasurfaces. This class of PCSs is composed of multiple printed dielectric layers stacked together to impose localized time-delay throughout the aperture of the antenna. The second generation of PCSs have been successful in replicating almost the same electromagnetic performance as that of the first; nevertheless, the presence of multiple fairy large dielectric substrates and the associated bonding techniques contribute to an expensive antenna system, limiting

A. Lalbakhsh is with the School of Engineering, Macquarie University, Sydney, NSW 2109, Australia, and also with CSIRO Astronomy and Space Science, P.O. Box 76, Epping, NSW 1710, Australia (e-mail: ali.lalbakhsh@mq.edu.au, lalbakhsha@gmail.com).

K. P. Esselle and Muhammad U. Afzal are with the School of Electrical & Data Engineering, University of Technology Sydney, Sydney, Australia (e-mail: muhammad.afzal@uts.edu.au, Karu.Esselle@uts.edu.au).

S. L. Smith is with CSIRO Astronomy and Space Science, P.O. Box 76, Epping, NSW 1710, Australia (e-mail: stephanie.smith@csiro.au).

Color versions of one or more of the figures in this paper are available online at http://ieeexplore.ieee.org.

XXX XX, 20XX; revised XXXX XX, 20XX.

its applications in highly specialized practices.

Reviewing literature reveals that while there has been a promising trajectory on evolution of PCSs for aperture antennas like ERAs, the critical aspect of market affordability has been overlooked, posing a serious barrier for ERAs to find their applications in today's industry. This paper introduces the third generation of the PCSs, where industrial justification and cost is equally weighted along with the electromagnetic performance. Here, in the third generation of PCS, dielectric substrates are made redundant for the first time, making a breakthrough in relation to the fabrication cost, while the electromagnetic performance is not sacrificed and comparable with the previous high-cost generations. Additionally, all-metal configurations are preferred in high-power applications as discussed in [21]. The proposed All-Metallic PCS (AMPCS) is made of three stainless steel surfaces segregated with a sub-wavelength air-gap, without the need for any bonding techniques, as opposed to all other classes of PCS which either require thick dielectric thicknesses, or multiple of expensive printed RF laminates. It is well-known that the existence of dielectric materials in an EM structure will introduce additional loss, which depends on the inherent dissipation of electromagnetic energy of the materials as well as frequency. This additional loss can be minimized at the significant increased cost of development, but cannot be eliminated. We have developed a PCS which does not use any dielectric material at all to eliminate these additional losses.

It should be noted that the proposed AMPCS can be made of different types of metal through a variety of fabrication techniques, such as laser cutting or stamping a thin metal sheet, opening a new door to affordable large-scale prototyping, which was otherwise not possible with the expensive commercial RF laminates. Additionally, the AMPCS is lightweight and has no limitations in terms of polarizations, due to its symmetrical topology both in macroscopic and microscopic levels.

The rest of this paper is organized as follows. Section II describes briefly the phase defect of a typical ERA and suggest the macroscopic and microscopic configurations of the AMPCS. Section III discusses the fabrication process of the proposed AMPCS and some special considerations need to be taken into account for metal manufacturing. Section IV presents the near-field and far-field results of the antenna system, highlighting the AMPCS performance.

II. Design of the AMPCS

The design procedure of AMPCS can be divided into two major steps, in which a macroscopic configuration of the AMPCS is firstly suggested based on the nature of the near-field non-uniformity of the electromagnetic (EM) source under examination. To do so, an ERA is used as an example case of an aperture EM source suffering from a highly spherical wavefront. In the second step, microscopic topology needs to be discussed, where the configurations of all-metal phase-correcting elements are proposed.

A. Macroscopic topology of the metallic PCS

A conventional ERA is composed of a partially reflecting surface (PRS) placed at a half wavelength from a ground plane containing a simple feed. The feed excites the cavity formed between the PRS and the ground plane [3]. In a different approach, fully reflecting surfaces can also be engineered to form an ERA as explained in [22]–[24]. Fig. 1(a) shows the ERA under examination with a flat unprinted surface as its PRS. The PRS is made of Rogers TMM 4 with a thickness of 3.17 mm, which is close to $\lambda_g/4$, as recommended in the literature [3], [7], and placed at a distance of $\lambda_0/2$ from the ground plane to construct a cavity, where λ_0 and λ_g are the free-space wavelength and guided wavelength within the PRS at the operating frequency of 11 GHz. The cavity was excited using a single slot antenna with an opening of 13.2 mm$\times$8 mm placed in the center of the ground. In order to calculate the phase errors in the antenna aperture originated from the transversal prorogation of the slot antenna, an imaginary plane is considered at a sub-wavelength distance of 7 mm from the antenna where the local phase values are measured and depicted by a 2D plot in Fig. 1(b). As can be seen from this plot, the near-field phase values are approximately independent with respect to ϕ in the cylindrical coordinates.

In order to discretize the aperture phase distribution, the actual phase values along the $\phi = 0$, with an interval of $\lambda_0/3$ are captured in the imaginary plane, resulting in 7 discrete values, which are used to quantify the aperture phase-errors with respect to an arbitrary constant. The sampling interval is critical and chosen following the recommendations in [9], [14], [25], [26], as large intervals would result in sub-optimal correction, due to discretization error and too small ones would cause fabrication complexity, especially for an all-metal structure. To correct such circularly symmetrical, yet highly non-uniform, phase distribution of the antenna, the proposed AMPCS needs to follow the same symmetry, resulting in a semi-rotational orientation of 7 different phase-correcting elements, as shown in Fig. 2. It should be noted that such arrangement is not singular and any other circular patterns inspired by the actual near-field phase distribution of the EM source can be used. Knowing the macroscopic structure of the AMPCS and the required localized phase correction, next step is to design phase-correcting elements of the AMPCS.

B. Microscopic topology of AMPCS

The Second generation of PCSs are generally composed of localized spatial phase shifters developed by stacking multiple expensive RF laminates. The use of dielectric as a substrate for the metallic patterns along with a wide variety of available substrates (numerous dielectric constants and thicknesses) provides PCS designers with an extremely large degree of freedom to achieve the transmission properties required throughout the PCSs [12], [13], [15], [16], [27], [28]. Indeed, any conductive patterns, resonant or non-resonant elements, with any commercially available substrates can be used to achieve a transparent structure with the required phase delay at the operating frequency. On the other hand, such flexibility does not exist with all-metal configurations. Therefore, non

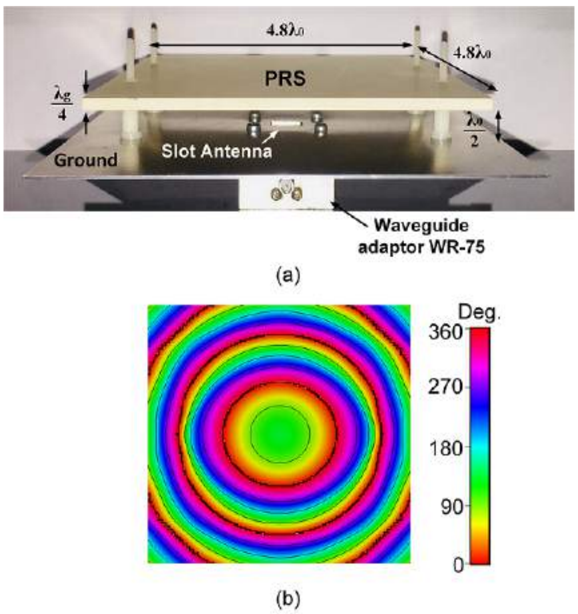

Fig. 1. (a) A photo of the fabricated ERA with an unprinted PRS made of Rogers TMM 4. (b) 2D presentation of the phase distribution of E_y 7 mm above the antenna aperture.

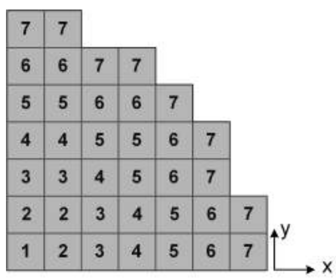

Fig. 2. Quasi-circular arrangement of the phase-correcting elements used for the AMPCS realization.

of the proposed configurations of printed phase-correcting elements in the literature can be implemented in a fully metallic topology.

To tackle this issue, we propose a hybrid all-metal configuration for the phase-correcting elements, in which different number of segregated conductive layers are used. In the proposed configuration, the consistency and the mechanical integrity, which are the main barriers to the all-metal EM devices, are ensured by an inductive metallic grid extending throughout AMPCS structure. The justification to use such a high-impedance metallic network is grounded by the fact that the resonance condition can be potentially satisfied by a combination of the inductive effects of two segregated metallic grids and the capacitive effects of the transmission line placed between the two grids. Consequently, it can be hypothesized that a pair of inductive grids will create a high-transmission window around their resonance, making them a possible phase-correcting element, in addition to their primary role of ensuring mechanical consistency of other metallic patterns used in the future phase-correcting elements.

To verify this hypothesis, a parametric analysis of two identical metallic grids separated by 10 mm ($\approx \lambda_0/3$) with

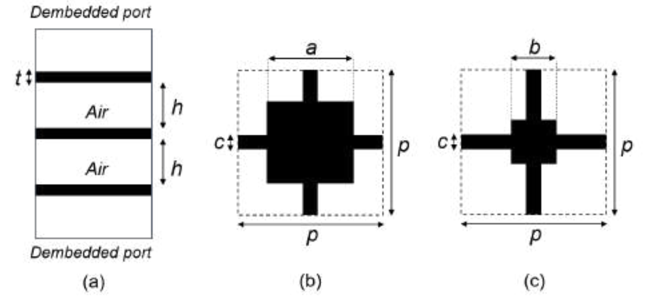

Fig. 3. Unit-cell configuration of the all-metal phase shifters used in Ring 2 to Ring 7 of the quasi-circular geometry shown in Fig. 2 (a) Side view of a unit cell of the AMPCS. (b) Top and bottom conductive patterns of a unit cell of the AMPCS. (c) The middle conductive pattern of a unit cell in the AMPCS. In each unit cell, the square paths are held by the inductive strips with a constant width of c. The inductive strips running throughout the the three surfaces, responsible for the integrity of the structure.

varying widths from 0.4 mm to 1.6 mm and a step of 0.1 mm was carried out using CST MWS. According to the numerically computed transmission coefficients, a phase range of 100 degrees ($125°$ to $225°$) with reasonably high transmission magnitude can be achieved by this simple structure. The significance of this relatively small phase range will be revealed when other phase-correcting topologies are designed and appear to fail to fill the same phase-range.

To achieve other required phase-delay values, metallic patches are incorporated into three layers of the metallic grid, creating new phase-correcting elements, as illustrated in Fig. 3. The size of each element is set to $\lambda_0/3$ and denoted by p in Fig. 3. To ensure reciprocity and simplicity of the proposed AMPCS, the top and bottom patches are designed to be identical with a maximum size of $p = \lambda_0/3$. In this configuration, the width of the grid and the thickness of both patches and girds are set to 0.4 mm and 1 mm, respectively, considering the limitations associated to the laser cutting which is used in the fabrication process and discussed in Section Section III. The size of the square patches, however, are varied to achieve the required phase shifts using a parametric study with a step size of 0.3 mm chosen based on the fabrication tolerance.

The transmission phase and magnitude at the operating frequency of 11 GHz are extracted from the parametric study and illustrated through a polar graph shown in Fig. 4. In this plot, the transmission characteristics of each phase-correcting element is presented by a blue square, suggesting the incapability of the unit-cell configuration in Fig. 3 in covering the phase values of $45°$ to $210°$, which would be a barrier for the phase correction of EM sources with a severe aperture phase non-uniformity like the ERA under consideration. This problem is rectified by using a pair of standalone inductive grids as phase-correcting elements, as explained earlier, and shown by red crosses in Fig. 4.

The final stage of designing AMPCS is choosing the suitable candidates from the element bank shown in Fig. 4 and arrange them in the pre-designed macroscopic regime discussed in Section II-A, in which only 7 discrete correcting elements are required. The geometrical and EM properties of the unit cells used in the APMCS are tabulated in Table I. As shown

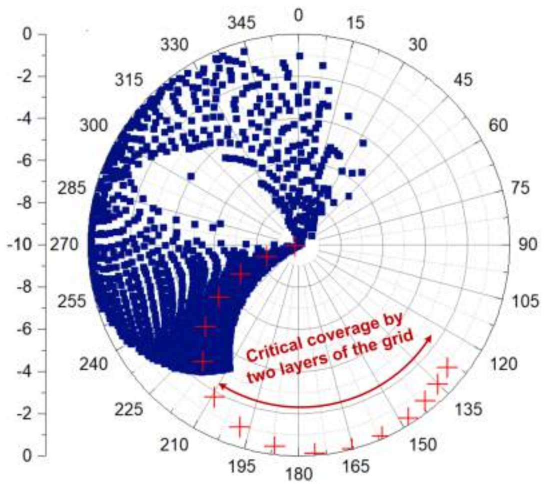

Fig. 4. Polar representation of the transmission coefficients generated by the proposed hybrid all metal configuration. The blue squares represent the transmission components of three square patches connected by the three layers of the metallic grid. Red crosses show the transmission coefficients of two layers of the grid in the absence of metallic patches.

TABLE I
GEOGRAPHICAL AND ELECTROMAGNETIC PROPERTIES OF THE PHASE CORRECTING ELEMENTS USED IN THE AMPCS

Ring no.	$\|S21\|$ (dB)	$\Delta\phi$ (Deg.)	No. of metallic Layers	a (mm)	b (mm)	c (mm)
1	0.0	187	2	0	0	0.8
2	-2.7	214	3	0	2.7	0.4
3	-0.1	255	3	0	6.2	0.4
4	-0.2	296	3	3.3	6.2	0.4
5	-0.5	330	3	5.4	5.5	0.4
6	-0.5	330	3	5.4	5.5	0.4
7	-3.0	12	3	6.8	4.8	0.4

Note: Ring no. corresponds to the quasi-circular arrangement of the phase-correcting elements illustrated in Fig. 2. Letters a, b and c correspond to the geometry depicted in Fig. 3, where a is the size of the top and bottom patches, b is the middle patch size, and c is the grid width.

in the table, the first correcting ring (Ring 1) is composed of only two layers of grid, while Ring 2 and 3 consist of three layers of grid and one middle patch, all other correcting rings require 3 metallic patches. It needs to be mentioned that the unit cell used in Ring 7 is slightly less transparent than other phase-correcting cells, however it should not affect the overall performance of the antenna system, as the magnitude of aperture field is considerably weaker in outermost areas.

The proposed design technique is distinguished from other PCB PCSs reported in [12] and [13] at different levels. Firstly, all other PCB PCSs mentioned above are composed of metallic patches printed on multiple layers of microwave substrates. Such geometries are impossible to implement using a dielectric-free structure, and hence cannot be used in the AMPCS. Secondly, in the AMPCS, the phase range required for the ERA phase correction is achieved using a hybrid structure, in which unit cells with different number of conductive layers and patterns are used, as opposed to the above-mentioned design, where only one geometry with the same number of layers are used.

III. Fabrication Considerations

There are a variety of fabrication methods which can be employed for realization of the proposed AMPCS, thanks to the recent advancements in the metal manufacturing technology. There are five possible prototyping procedures including Computer Numerical Control (CNC) machining [29], plasma cutting [30], metal additive manufacturing [31], waterjet cutting [32] and laser cutting [33]. Amongst them, we highly recommend the last two methods for the AMPCS prototyping. Indeed, the sharp vertex of the perforated polygons cannot be achieved using CNC machining, due to the round tip of CNC bits, additionally there is a high chance of metal failure during drilling because of the small thickness of the metal sheet. Secondly, plasma cutting performs efficiently only for large cutting areas with simple patterns, while the AMPCS has many miniature segments which would be damaged due to the destructive influence of plasma cutting on the confluences. Metal additive manufacturing is a very precise method for prototyping metallic objects with delicate segments; however, it is not recommended in the case of AMPCS, as the 3D printed AMPCS would be highly subject to damage, when it is removed from the printer bed, due to its small thickness. Either water-jet cutting and laser cutting can be used to fabricate the proposed AMPCS, as both method are capable to finely perforate metal sheets; nevertheless, the water-jet cutting is a lengthier process than laser cutting, leading to a higher fabrication cost, hence the AMPCS was fabricated using laser cutting technology.

The proposed AMPCS was made of stainless steel sheets using cutting-edge laser technology. The thickness of the metallic sheets plays a critical role in both fabrication and durability of the AMPCS. From the packaging points of view, greater thickness is preferred, as it is more sustainable and removes the need for any extra supports, such as radome or foam substrate. However, increase in the metal thickness would escalate the chance of metal failure during the fabrication process, due to the excessive heat absorbed by the thick metal sheet. Therefore, there is a trade-off which needs to be addressed at the beginning of the design process. In this design, the thickness of 1 mm is recommended considering the large volume of perforation performed on each surface of the AMPCS. Such selection ensures both fabricability and robustness of the freestanding AMPCS.

IV. Near-field and Far-field Results

Fig. 5 shows three layers of the AMPCS fabricated by a laser cutting machine (HL-6060C) with a maximum line cutting speed of 800 mm/s. The layers are separated with 4 nylon spaces to form the AMPCS, and placed on the antenna at a distance of $\lambda_0/4$ from the PRS, as depicted in Fig. 6. The reason for choosing $\lambda_0/4$ space between PRS and the AMPCS is because the local phase values of the electric aperture field of the antenna are captured on an imaginary plane at the same distance from the PRS, and hence the AMPCS is expected

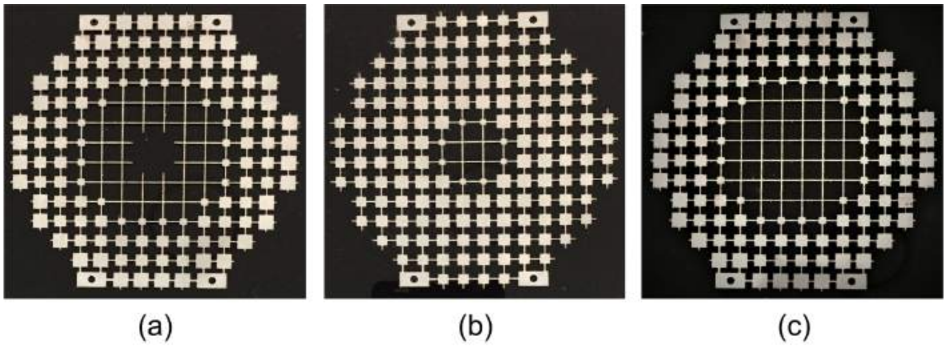

Fig. 5. Laser cut AMPCS made of stainless steel sheet with a thickness of 1 mm.(a) top layer, (b) middle layer, (c) bottom layer.

Fig. 6. A prototype of the fabricated AMPCS loaded on the ERA.

to have its optimum performance at this distance from the radiating aperture. It should be mentioned that the presented design procedure of AMPCS is not dependent of the PRS, and can be applied on ERAs regardless of their types of PRS.

The near electric field of the antenna system was numerically calculated using the time-domain solver of CST Microwave Studio (CST MWS) and shown in Fig. 7. It can be seen that a remarkable enhancement in the aperture phase distribution of the antenna system is achieved, extending the uniform phase region to more than double. The uniform phase region is referred to the area of the antenna aperture with a phase error smaller than 50 degrees [13].

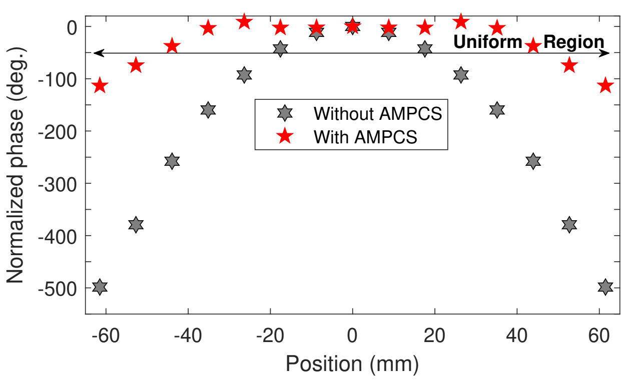

Fig. 7. Phase distribution of the y-component of the electric field of the ERA under consideration at 11 GHz. Uniform phase region is more than doubled due to AMPCS.

The input reflection coefficient of the ERA was simulated and measured using CST MWS and Agilent PNA-X N5242A vector network analyzer, respectively and plotted in Fig. 8.

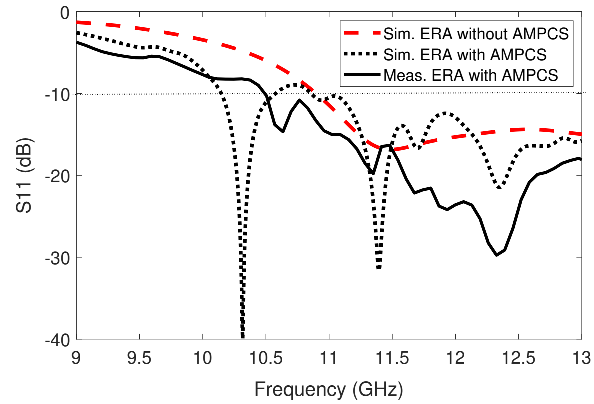

Fig. 8. Input reflection coefficient of the antenna.

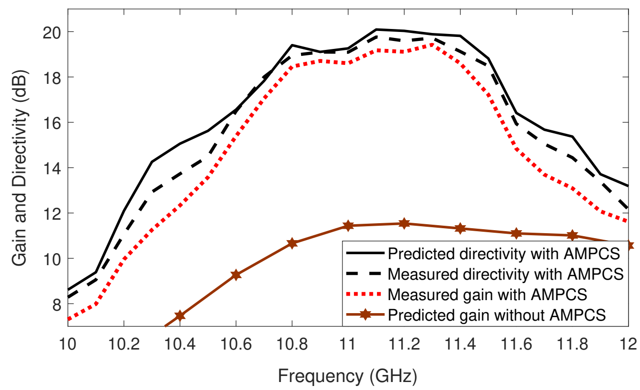

Fig. 9. A comparison between the gain and directivity of the ERA with and without the AMPCS.

According to the measured results, the 10 dB $|S11|$ bandwidth of the antennas with AMPCS is 42% from 10.6 to 16.3 GHz, which is in good agreement with the predicted values from CST MWS. Far-field peak gain and directivity of the ERA with AMPCS were measured in the Near-field Systems Inc. spherical near-field range, and compared with the predicated results in Fig. 9, verifying a significant improvement of 8.4 dB in the peak gain of the antenna, reaching to 19.42 dB at 11.3 GHz. According to the measurement, the 1 dB directivity and gain bandwidths are 6.4% and 5.9%, respectively, verifying stable far-field performance of the antenna system in a typical

TABLE II
COMPARISON WITH A FEW RECENTLY PROPOSED PCS

Reference number	No. of microwave substrates	Prototyping cost	Weight (g)	Peak gain (dB)	1dB Gain bandwidth (%)
[12]	3	Very high	190	19.3	≈ 3%
[13]	3	Very high	193	20.7	2.7 %
[15]	3	Very high	—	19.9	3.2%
[9]	8	Very high	335	20.2	≈ 3%
This work	None	Very low	87	19.4	5.9 %

frequency band required for Ku-Band applications.

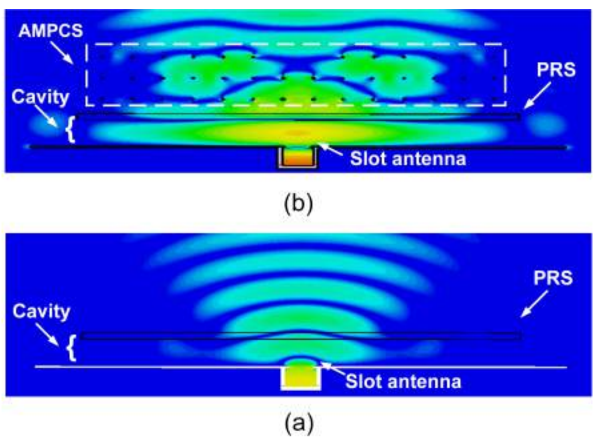

Fig. 10. A visualized comparison between the E-plane electric field distribution of the antenna, (a) in the absence of AMPCS, (b) in the presence of the AMPCS.

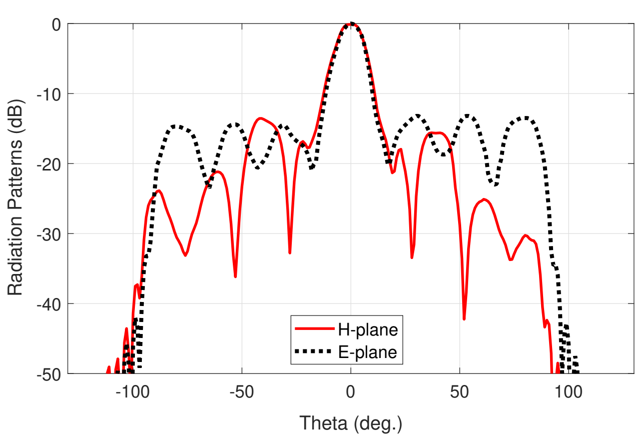

Fig. 11. Measured radiation patterns of the ERA under the APMCS loading.

The improved directivity and gain of the ERA with the AMPCS is achieved due to the enhanced phase distribution of the antenna aperture, which can be seen from the visualized electric field radiation in the E-plane, shown in Fig. 10. This radiation snapshot depicts the transformation of the spherical wavefront to a nearly planar wavefront of the E_y, significantly increasing the aperture efficiency of the antenna from 4% to 28%, because of the AMPCS. The transparency of the AMPCS can be estimated by inspecting the colors representing the intensity of the electric field at the input and output of the AMPCS in Fig. 10. It can be observed that there are almost same colors (intensity) below and above the AMPCS, exhibiting a good transmission properties in addition to the phase correction. Radiation patterns of the antenna in two principal planes are plotted in Fig. 11 showing, SLLs of -13.2 and -13.5 dB in the E- and H-planes, respectively, suggesting around 8 dB improvement in the SLLs in the E-plane over the Bare ERA.

V. CONCLUSION

An industrially-justified approach has been proposed in this paper to rectify the near-field non-uniformity associated with the aperture antennas and successfully tested with an ERA. Unlike the first and second generations of the PCS, the proposed AMPCS neither requires expensive microwave substrates nor any bonding techniques, resulting in a substantially lower fabrication cost, removing the main industrial barrier to the ERAs applications. A prototype of AMPCS was fabricated using available laser cutting technology and placed at a sub-wavelength distance from the ERA. The AMPCS has significantly compensate the non-uniform phase-delay of the antenna aperture, resulting in a considerable increase of 8.4 dB in the peak gain of the antenna, reaching a peak gain of 19.42 with a 1 dB gain bandwidth of around 6%. The measured radiation patterns are quite stable with SLLs better than -13 in both E- and H- plane, respectively. The proposed freestanding AMPCS does not need any mechanical support or protection and can be used for other aperture antennas for near-field enhancement.

REFERENCES

[1] D. I. de Villiers and S. M. Koziel, “Fast multi-objective optimisation of pencil beam reflector antenna radiation pattern responses using kriging,” *IET Microwaves, Antennas & Propagation*, vol. 12, no. 1, pp. 120–126, 2017.

[2] K. Konstantinidis, A. P. Feresidis, and P. S. Hall, “Multilayer partially reflective surfaces for broadband fabry-perot cavity antennas,” *IEEE Transactions on Antennas and Propagation*, vol. 62, no. 7, pp. 3474–3481, 2014.

[3] C. Cheype, C. Serier, M. Thèvenot, T. Monédière, A. Reineix, and B. Jecko, “An electromagnetic bandgap resonator antenna,” *IEEE Trans. Antennas Propag.*, vol. 50, no. 9, pp. 1285–1290, 2002.

[4] M. Akbari, S. Gupta, M. Farahani, A. Sebak, and T. Denidni, “Gain enhancement of circularly polarized dielectric resonator antenna based on fss superstrate for mmw applications,” *IEEE Trans. Antennas Propag.*, vol. 64, no. 12, pp. 5542–5546, 2016.

[5] M. Akbari, H. A. Ghalyon, M. Farahani, A.-R. Sebak, and T. A. Denidni, “Spatially decoupling of CP antennas based on FSS for 30-GHz MIMO systems,” *IEEE Access*, vol. 5, pp. 6527–6537, 2017.

[6] K. Konstantinidis, A. P. Feresidis, and P. S. Hall, “Broadband sub-wavelength profile high-gain antennas based on multi-layer metasurfaces,” *IEEE Transactions on Antennas and Propagation*, vol. 63, no. 1, pp. 423–427, 2015.
[7] L. Leger, R. Granger, M. Thevenot, T. Monediere, and B. Jecko, “Multifrequency dielectric ebg antenna,” *Microwave and Optical Technology Letters*, vol. 40, no. 5, pp. 420–423, 2004.
[8] A. Feresidis and J. Vardaxoglou, “A broadband high-gain resonant cavity antenna with single feed,” in *Antennas and Propagation, 2006. EuCAP 2006. First European Conference on*. IEEE, 2006, pp. 1–5.
[9] M. U. Afzal, K. P. Esselle, and B. A. Zeb, “Dielectric phase-correcting structures for electromagnetic band gap resonator antennas,” *IEEE Trans. Antennas Propag.*, vol. 63, no. 8, pp. 3390–3399, 2015.
[10] A. Lalbakhsh, M. U. Afzal, B. A. Zeb, and K. P. Esselle, “Design of a dielectric phase-correcting structure for an ebg resonator antenna using particle swarm optimization,” in *Proc. Int. Symp. Antennas Propag., Hobart, Australia*, 2015.
[11] A. Lalbakhsh, M. U. Afzal, K. P. Esselle, and S. L. Smith, “Wideband near-field correction of a fabry-perot resonator antenna,” *IEEE Transactions on Antennas and Propagation*, vol. 67, no. 3, pp. 1975–1980, 2019.
[12] M. U. Afzal and K. P. Esselle, “A low-profile printed planar phase correcting surface to improve directive radiation characteristics of electromagnetic band gap resonator antennas,” *IEEE Trans. Antennas Propag.*, vol. 64, no. 1, pp. 276–280, 2016.
[13] A. Lalbakhsh, M. U. Afzal, and K. P. Esselle, “Multi-objective particle swarm optimization to design a time delay equalizer metasurface for an electromagnetic band gap resonator antenna,” *IEEE Antennas Wireless Propag. Lett.*, vol. 16, pp. 912–915, 2017.
[14] M. U. Afzal, K. P. Esselle, and A. Lalbakhsh, “A methodology to design a low-profile composite-dielectric phase-correcting structure,” *IEEE Antennas Wireless Propag. Lett.*, vol. 17, no. 7, pp. 1223–1227, 2018.
[15] L. Zhou, X. Chen, X. Duan, and J. Li, “Fabry-perot antenna using a three-layer phase shifting structure for gain enhancement,” *IET Microwaves, Antennas & Propagation*, vol. 12, no. 3, pp. 400–405, 2017.
[16] P. Feng, X. Chen, and K. Huang, “High performance resonant cavity antenna with non-uniform metamaterial inspired superstrate,” *International Journal of RF and Microwave Computer-Aided Engineering*, vol. 27, no. 7, p. e21114, 2017.
[17] Y. Zheng, J. Gao, Y. Zhou, X. Cao, H. Yang, S. Li, and T. Li, “Wideband gain enhancement and rcs reduction of fabry–perot resonator antenna with chessboard arranged metamaterial superstrate,” *IEEE Trans. Antennas Propag.*, vol. 66, no. 2, pp. 590–599, 2018.
[18] L. Zhou, X. Chen, and X. Duan, “High gain fabry-perot cavity antenna with phase shifting surface,” in *Wireless Information Technology and Systems (ICWITS) and Applied Computational Electromagnetics (ACES), 2016 IEEE/ACES International Conference on*. IEEE, 2016, pp. 1–2.
[19] B. Ratni, W. A. Merzouk, A. de Lustrac, S. Villers, G.-P. Piau, and S. N. Burokur, “Design of phase-modulated metasurfaces for beam steering in fabry–perot cavity antennas,” *IEEE Antennas and Wireless Propagation Letters*, vol. 16, pp. 1401–1404, 2017.
[20] J. H. Kim, C.-H. Ahn, and J.-K. Bang, “Antenna gain enhancement using a holey superstrate,” *IEEE Transactions on Antennas and Propagation*, vol. 64, no. 3, pp. 1164–1167, 2016.
[21] X. Zhao, C. Yuan, L. Liu, S. Peng, Q. Zhang, and H. Zhou, “All-metal transmit-array for circular polarization design using rotated cross-slot elements for high-power microwave applications,” *IEEE Transactions on Antennas and Propagation*, vol. 65, no. 6, pp. 3253–3256, 2017.
[22] K. Dutta, D. Guha, and C. Kumar, “Synthesizing aperture fields over the superstrate of resonance cavity antenna for modifying its radiation properties,” *IEEE Antennas and Wireless Propagation Letters*, vol. 15, pp. 1677–1680, 2016.
[23] K. Dutta, D. Guha, C. Kumar, and Y. M. Antar, “New approach in designing resonance cavity high-gain antenna using nontransparent conducting sheet as the superstrate,” *IEEE Trans. Antennas Propag.*, vol. 63, no. 6, pp. 2807–2813, 2015.
[24] K. Dutta, D. Guha, and C. Kumar, “Theory of controlled aperture field for advanced superstrate design of a resonance cavity antenna with improved radiations properties,” *IEEE Transactions on Antennas and Propagation*, vol. 65, no. 3, pp. 1399–1403, 2017.
[25] N. Gagnon, A. Petosa, and D. A. McNamara, “Printed hybrid lens antenna,” *IEEE Transactions on Antennas and Propagation*, vol. 60, no. 5, pp. 2514–2518, 2012.
[26] N. Gagnon, A. Petosa, and D. McNamara, “Thin microwave quasi-transparent phase-shifting surface (pss),” *IEEE Transactions on Antennas and Propagation*, vol. 58, no. 4, pp. 1193–1201, 2010.
[27] K. K. Katare, A. Biswas, and M. J. Akhtar, “Microwave beam steering of planar antennas by hybrid phase gradient metasurface structure under spherical wave illumination,” *Journal of Applied Physics*, vol. 122, no. 23, p. 234901, 2017.
[28] K. K. Katare, A. Biswas, and J. Akhtar, “Wideband beam-steerable configuration of metasurface loaded slot antenna,” *International Journal of RF and Microwave Computer-Aided Engineering*, p. e21408, 2018.
[29] J. Valentino and J. Goldenberg, *Introduction to computer numerical control (CNC)*. Prentice Hall Englewood Cliffs, 2003.
[30] S.-I. Kim and M.-H. Kim, “Evaluation of cutting characterization in plasma cutting of thick steel ship plates,” *International Journal of Precision Engineering and Manufacturing*, vol. 14, no. 9, pp. 1571–1575, 2013.
[31] W. E. Frazier, “Metal additive manufacturing: a review,” *Journal of Materials Engineering and Performance*, vol. 23, no. 6, pp. 1917–1928, 2014.
[32] S. Srinivas and N. R. Babu, “Penetration ability of abrasive waterjets in cutting of aluminum-silicon carbide particulate metal matrix composites,” *Machining Science and Technology*, vol. 16, no. 3, pp. 337–354, 2012.
[33] S. Katayama, *Handbook of laser welding technologies*. Elsevier, 2013.

Ali Lalbakhsh received the B.S. and M.S degrees in electronic and telecommunication engineering from Islamic Azad University, Iran, in 2008 and 2011, respectively. He received the Master of Research degree (HD) and the Ph.D. in electronics engineering from Macquarie University, Australia in 2015 and 2020, respectively, and he is currently a sessional academic in the same institution. He has authored and co-authored around 60 peer-reviewed journal and conference papers so far. His research interests include resonance-based antennas, frequency selective surfaces, electromagnetic metasurfaces, periodic and electromagnetic band gap structures, evolutionary optimisation methods and microwave passive components.

Mr. Lalbakhsh received several prestigious awards including an international Research Training Program scholarship (iRTP) for the MRes, international Macquarie University Research Excellence Scholarship (iMQRES) for the PhD, Commonwealth Scientific and Industrial Research Organization (CSIRO) grants on Astronomy and Space exploration, Macquarie University Postgraduate Research Fund (PGRF) and WiMed Travel Support Grants. He was a recipient of the 2016 ICEAA-IEEE APWC Cash Prize and Macquarie University Deputy Vice-chancellor commendation in 2017.

Ali is the only researcher in IEEE Region 10 (Asia-Pacific) who has won the most prestigious Best Paper Contest of IEEE Region 10 more than once. He was awarded First, Second and Third Prices in this international competition in 2018, 2019 and 2016, respectively. He is nominated for the 2019 Excellence in Higher Degree Research Award-Science, Technology, Engineering, Mathematics and Medicine (STEMM) at Macquarie University.

Muhamamd U. Afzal (S'13–M'16) received the B.S. degree in electronics engineering (hons.) and Master degree in Computational Science and Engineering from National University of Sciences and Technology (NUST), Islamabad, Pakistan, in 2005 and 2011, respectively. He completed his PhD in electronics engineering from Macquarie University in 2016.

From 2010 to 2012, he was a lab engineer at Samar Mubarakmand Research Institute of Microwave and Millimeterwave Studies (SMRIMMS), Islamabad, Pakistan. From 2012 to 2013, he was a lecturer in the electrical engineering department, NUST, Islamabad, Pakistan. He is now a research fellow at University of Technology Sydney. His research interests include electromagnetic band gap or Fabry-Perot resonator antennas, high-gain planar metasurface based antennas, radial-line slot antennas, phased arrays, free-standing phase-shifting structures or metasurfaces, frequency selective surfaces, near-field phase transformation, and far-field pattern synthesis using near-field phase transformation.

Mr. Muhammad received NUST merit base scholarship during undergraduate studies and International Macquarie Research Excellence Scholarship (iMQRES) for PhD studies.

Karu P. Esselle (M'92–SM'96–F'16) is the Distinguished Professor in Electromagnetic and Antenna Engineering at the University of Technology Sydney and a Visiting Professor of Macquarie University, Sydney. According to a Special Report on Research published by The Australian national newspaper in 2019, he is the National Research Field Leader in Australia in Microelectronics and Electronic Packaging fields in Engineering Discipline as well as the Electromagnetism field in the Disciplines of Physics and Mathematics.

Karu received BSc degree in electronic and telecommunication engineering with First Class Honours from the University of Moratuwa, Sri Lanka, and MASc and PhD degrees with near-perfect GPA in electrical engineering from the University of Ottawa, Canada. Previously he was Director of WiMed Research Centre and Associate Dean – Higher Degree Research (HDR) of the Division of Information and Communication Sciences and directed the Centre for Collaboration in Electromagnetic and Antenna Engineering at Macquarie University. He has also served as a member of the Dean's Advisory Council and the Division Executive and as the Head of the Department several times.

In 2018 and again in 2019, Karu has been selected to chair the prestigious Distinguished Lecturer Program Committee of the IEEE Antennas and Propagation (AP) Society – the premier global learned society dedicated for antennas and propagation - which has about 9,000 members worldwide. After two stages in the selection process, Karu was also selected by this Society as one of two candidates in the ballot for 2019 President of the Society. Only three people from Asia or Pacific apparently have received this honour in the 68-year history of this Society. Karu is also one of the three Distinguished Lecturers (DL) selected by the Society in 2016. He is the only Australian to chair the AP DL Program ever, the only Australian AP DL in almost two decades, and second Australian AP DL ever (after UTS Distinguished Visiting Professor Trevor Bird). He has been continuously serving the IEEE AP Society Administrative Committee in several elected or ex-officio positions since 2015. Karu is also the Chair of the Board of management of Australian Antenna Measurement Facility, and was the elected Chair of both IEEE New South Wales (NSW), and IEEE NSW AP/MTT Chapter, in 2016 and 2017. Karu was elevated to prestigious IEEE Fellow grade for his contributions to resonance-based antennas. He is also a Fellow of Engineers Australia.

Karu has authored approximately 600 research publications and his papers have been cited over 8,500 times. In 2018 alone his publications received 1123 citations. He is the first Australian antenna researcher ever to reach Google Scholar h-index of 30 and his citation indices have been among the top Australian antenna researchers for a long time (in November 2019: i10 is 166 and h-index is 44). Since 2002, his research team has been involved with research grants, contracts and PhD scholarships worth about 20 million dollars, including 15 Australian Research Council grants, without counting the 245 million-dollar SmartSat Corporative Research Centre, which started in 2019. His research has been supported by many national and international organisations including Australian Research Council, Intel, US Air Force, Cisco Systems, Hewlett-Packard, Australian Department of Defence, Australian Department of industry, and German and Indian governments.

Karu's awards include 2019 Motohisa Kanda Award (from IEEE USA) for the most cited paper in IEEE Transactions on EMC in the past five years, selection as a Finalist for the forthcoming 2019 Macquarie University Research Excellence Awards for Innovative Technologies, 2019 ARC Discovery International Award, 2017 Excellence in Research Award from the Faculty of Science and Engineering, 2017 Engineering Excellence Award for Best Innovation, 2017 Highly Commended Research Excellence Award from Macquarie University, 2017 Certificate of Recognition from IEEE Region 10, 2016 and 2012 Engineering Excellence Awards for Best Published Paper from IESL NSW Chapter, 2011 Outstanding Branch Counsellor Award from IEEE headquarters (USA), 2009 Vice Chancellor's Award for Excellence in Higher Degree Research Supervision and 2004 Innovation Award for best invention disclosure. His mentees have been awarded many fellowships, awards and prizes for their research achievements. Forty-eight international experts who examined the theses of his recent PhD graduates ranked them in the top 5

Karu has provided expert assistance to more than a dozen companies including Intel, Hewlett Packard Laboratory (USA), Cisco Systems (USA), Audacy (USA), Cochlear, Optus, ResMed and Katherine-Werke (Germany). Among them, his team designed the high-gain antenna system for the world's first entirely Ka-band CubeSat made by Audacy, USA and launched to space by SpaceX in December 2018. This is believed to be the first Australian-designed high-gain antenna system in space, since CSIRO-designed antennas in Australia's own FedSat launched in 2002.

Karu is in the College of Expert Reviewers of the European Science Foundation (2019-22) and he has been invited to serve as an international expert/research grant assessor by several other research funding bodies as well, including European Research Council and national agencies in Norway, the Netherlands, Canada, Finland, Hong-Kong, Georgia, South Africa and Chile. He has been invited by Vice-Chancellors of Australian and overseas universities to assess applications for promotion to professorial levels. He has also been invited to assess grant applications submitted to Australia's most prestigious schemes such as Australian Federation Fellowships and Australian Laureate Fellowships. In addition to the large number of invited conference speeches he has given, he has been an invited plenary or keynote speaker of several IEEE and URSI conferences and workshops including URSI'19 Seville, Spain, and 23rd ICECOM in 2019 in Dubrovnik, Croatia.

He is an Associate Editor of IEEE Transactions on Antennas Propagation as well as IEEE Access. He is the Technical Program Committee Co-Chair of ISAP 2015, APMC 2011 and TENCON 2013 and the Publicity Chair of ICEAA 2016, IWAT 2014 and APMC 2000. His previous research activities are posted in the web at http://web.science.mq.edu.au/ esselle/ .

Stephanie L Smith (M'99) received the B.Eng (Hons) in microelectronic engineering and Ph.D. degrees from Griffith University, Australia, in 1995 and 2000 respectively. She joined the Commonwealth Scientific and Industrial Research organization (CSIRO) as a research scientist in 1999. She is currently a senior research scientist at CSIRO Astronomy and Space Science with interests in printed antennas, millimeter-wave antennas and passive components, three-dimensional integration and packaging, radio astronomy feeds and antenna measurement. Stephanie was Chair of the Australian Symposium on Antennas from 2009 to 2015.